

The above equations are solved and we find:

$$\begin{aligned} A_0^1 &= [1 - (\tau_0/2\tau_l)(1+C_-)]D_l^{-1}, \\ B_0^1 &= i(\tau_0/2\tau_l)E_+D_l^{-1}, \quad \text{for } l \neq 0, \end{aligned} \quad (\text{A3})$$

and

$$\begin{aligned} A_0^1 &= (1-C_-)(2D_-^{-1})^{-1}, \\ B_0^1 &= iE_+(2D_-^{-1})^{-1}, \quad \text{for } l=0, \end{aligned} \quad (\text{A4})$$

where

$$D_l = 1 - (\tau_0/\tau_l) + O(\tau\Delta), \quad (\text{A5})$$

and

$$D_-^{-1} = \tau\Delta[(1+u^2)^{1/2} + (1+u_+^2)^{1/2} - \zeta(1-C_-)]. \quad (\text{A6})$$

From the above expressions we see that the term pro-

portional to $\tau\Delta\zeta$ in Eq. (A1) gives negligible correction (of the order of $\tau\Delta$) for the case of $l \neq 0$ while it gives an important contribution in the case of $l=0$. We obtain almost similar equations for the other amplitudes $\{A_i^1, B_i^1\}$ ($i \neq 0$).

Now let us turn to the case of nonvanishing q . In this case we obtain equations similar to those in (A1), which can be obtained by simply replacing $\Omega(\omega)^{-1}$ by $\Omega(\omega)^{-1}(lq)^{-1} \arctan(q/l)$ for the s -wave case. In a higher wave vertex such a momentum dependence is negligible as long as $ql \ll 1$.

In the case of paramagnetic impurities the equations involved are much more simple and we do not feel it is necessary to present them here.

Linewidth of the Electron Paramagnetic Resonance of $(\text{Al}_2\text{O}_3)_{1-x}(\text{Cr}_2\text{O}_3)_x$ †

RICHARD F. WENZEL AND YEONG W. KIM

Department of Physics, Wayne State University, Detroit, Michigan

(Received 13 July 1965)

The linewidth variation of electron-paramagnetic-resonance (EPR) absorption in single crystals of $(\text{Al}_2\text{O}_3)_{1-x}(\text{Cr}_2\text{O}_3)_x$ with x equal to 0.01, 0.001, or 0.0001% has been investigated as a function of the angle between the C axis of the samples and the magnetic field. The observed width variation is practically independent of the values of x and of the choice of the axis of rotation perpendicular to both the C axis and the magnetic field. In order to account for the observed width variation, three alternative models have been considered: a mosaic model, a strain model, and a hybrid of the two models. The calculated width variation based on each of the three models is in qualitative agreement with the observed one, the degree of agreement being the best for the strain model. Quantitatively, however, significant discrepancies between the observed and calculated variations have been found for some regions of the angle of rotation. Some discussions of the discrepancies are presented.

I. INTRODUCTION

RECENT electron-paramagnetic-resonance (EPR) absorption studies^{1,2} of the Cr^{3+} ion in single crystals of $(\text{Al}_2\text{O}_3)_{1-x}(\text{Cr}_2\text{O}_3)_x$ with x close to 0.03% have indicated that the width of the three EPR lines corresponding to the $(\frac{1}{2} \rightarrow -\frac{1}{2})$ and $(\frac{3}{2} \rightarrow \frac{1}{2})$ transitions is approximately 12 G, when the external magnetic field is parallel to the crystallographic (111) or C axis of the samples. For such small values of x , the spin-spin interactions among the Cr ions contribute insignificantly to the linewidth. For example, when x is taken to be 0.001%, the linewidth of the $(\frac{3}{2} \rightarrow \frac{1}{2})$ transition, if broadened solely by the spin-spin interaction, would be not larger than 0.5 G.¹ Under the circumstances, the hyperfine interactions between the electronic spin of each Cr ion and its neighboring Al²⁷ nuclei of spin $\frac{5}{2}$ and of 100% abundance have to be considered as being

responsible for the linewidth. According to Laurance *et al.*,² the hyperfine broadening mechanism would lead to a linewidth of 9.7 G. This is approximately 81% of the observed width of 12 G. Thus the hyperfine broadening mechanism appears to be the major, but not the sole, source of the linewidth for the case of the magnetic field being parallel to the C axis.

The linewidth is expected to vary depending upon the angle θ between the C axis and the magnetic field if the dipolar part of the hyperfine interactions is appreciable. The expected anisotropy of the linewidth may be calculated in terms of the hyperfine coupling constants measured by Laurance *et al.*² The hyperfine broadening mechanism then would predict a variation of the linewidth between 9.4 and 9.9 G [see Eq. (B 14) of Ref. 1], when the samples are rotated over the 90° range of θ about an axis which is perpendicular to the C axis. In the following, the axis of rotation is referred to as the a axis.

However, the experimental results obtained from the sample with x less than 0.01% investigated in the present work indicate that the linewidth varies by approximately a factor of 5 over the 90° range of θ ,

† Work supported by U. S. Atomic Energy Commission Contract No. AT(11-1)-1054.

¹ W. J. C. Grant and M. W. P. Strandberg, *Phys. Rev.* **135**, A715 (1964); **135**, A727 (1964).

² N. Laurance, E. C. McIrvine, and J. Lambe, *J. Phys. Chem. Solids* **23**, 515 (1962).

and also that the angular dependence of the width is not the same for individual EPR lines. Thus, the hyperfine broadening mechanism alone is not capable of fully accounting for the experimental results.

In order to understand this discrepancy, three different models are considered. In the first, the samples are viewed as being in the form of a mosaic of microcrystals. In the second model, the system is viewed as having random localized strains. The third model is a hybrid of the above two models. The mosaic model is similar in nature to the model employed by Shaltiel and Low³ for the case of Gd in ThO₂, and the strain model to that used by Feher⁴ to explain the broadening of Mn and Fe absorption lines in MgO.

Elementary theories of the mosaic and strain models are given in the following section. The experimental results and discussions are presented in Sec. III and a conclusion is drawn in the last section.

II. ELEMENTARY THEORIES

The magnetic-energy-level structure of a Cr³⁺ ion in single crystals of (Al₂O₃)_{1-x}(Cr₂O₃)_x has been conveniently described in terms of an axially symmetric spin Hamiltonian^{1,2,5-7}

$$\mathcal{H} = g_{\parallel} \beta S_z H_z + g_{\perp} \beta S_x H_{\perp} + D(S_z^2 - \frac{5}{4}), \quad (1)$$

where the z axis is the axis of symmetry, which is the C axis of the sample, and S stands for an effective spin of $\frac{3}{2}$. The two subscripts \parallel and \perp mean "parallel" and "perpendicular" to the z axis, respectively. The values of the constants in Eq. (1) are as follows:

$$g_{\parallel} = 1.9840, \\ g_{\perp} = 1.9867^{5,6},$$

and

$$D = -5.75 \text{ kMc/sec.}^7 \quad (2)$$

When the resonance condition is established with a fixed microwave frequency ν_0 , and a slowly swept magnetic field, the EPR lines are observed at certain values of the magnetic field, which vary depending upon the value of θ . The curves in Fig. 1 represent an experimental plot of H versus θ for the EPR lines observed from a sample with $x=0.001\%$ for the value of ν_0 equal to 9.472 kMc/sec (see also Sec. III). Because of the fixed microwave frequency ν_0 , the curves will be referred to as the isofrequency curves for convenience in the following. The magnetic levels, the resonance transitions, and the isofrequency curves are labeled in accordance with the conventions employed by Weber,⁸ with

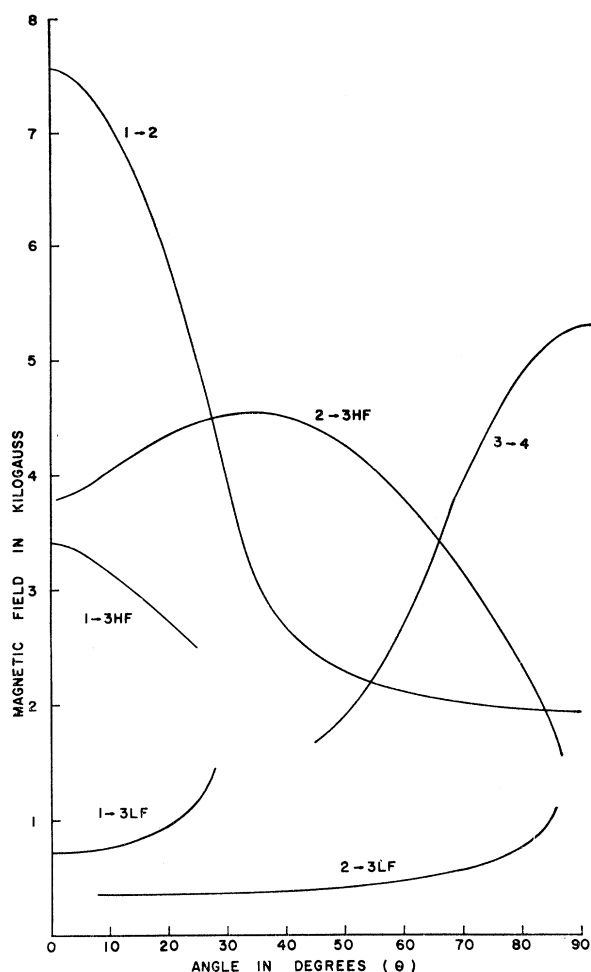


FIG. 1. The isofrequency curves of the EPR lines of the Cr³⁺ ions in (Al₂O₃)_{1-x}(Cr₂O₃)_x with $x=0.001\%$ for the microwave frequency $\nu_0=9.472$ kMc/sec. The four energy levels of the ions are labeled, 1, 2, 3, and 4 from the highest level down (see Ref. 8). Thus the curve (1-2) corresponds to the transition between the levels 1 and 2. The notations HF and LF are used to distinguish two EPR lines, one at higher field (HF) and the other at lower field (LF), pertaining to a pair of levels. Portions of the curves (1-3), (2-3), and (3-4) are missing for some values of θ , because the corresponding transitions are either forbidden or yield almost unobservable EPR lines.

the proper correction for the sign of D in Eq. (1).

If the sample is crystallographically "perfect," the local C axes passing through the sites of the Cr ions are all parallel among themselves, and should make the same angle with the magnetic field. The common direction of the local C axes is then the direction of the C axis of the perfect sample. Also D in Eq. (1) is the same for all Cr ions and the z direction used in Eq. (1) is along the crystallographic C axis. Thus the magnetic levels, and consequently the resonant magnetic field positions of the EPR lines, are coincident for all the Cr ions. This means that the width of the EPR lines observed from the perfect sample should be identical to

³ D. Shaltiel and W. Low, Phys. Rev. **124**, 1062 (1961).

⁴ E. R. Feher, Phys. Rev. **136**, A145 (1964).

⁵ A. A. Manenkov and A. M. Prokhorov, Zh. Eksperim. i Teor. Fiz. **28**, 762 (1955) [English transl.: Soviet Phys.—JETP **1**, 611 (1955)].

⁶ M. Zaripov and I. Shamonin, Zh. Eksperim. i Teor. Fiz. **30**, 291 (1956) [English transl.: Soviet Phys.—JETP **30**, 291 (1956)].

⁷ J. E. Geusic, Phys. Rev. **102**, 1252 (1956).

⁸ J. Weber, Rev. Mod. Phys. **31**, 681 (1959).

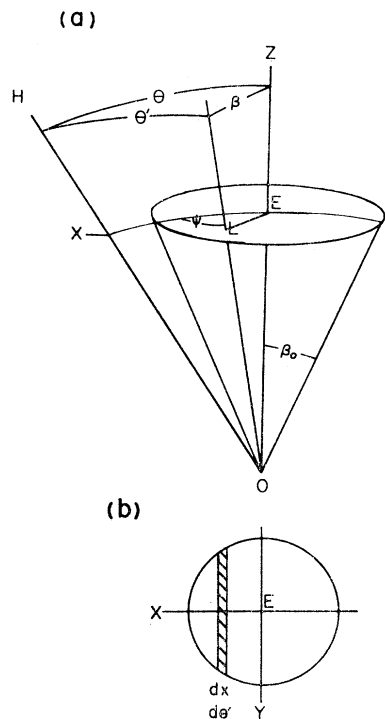


FIG. 2. (a) The coordinate system for the mosaic model. The direction of the C axis (OL) of a perfect microcrystal is specified by the angles β and ψ on the unit sphere centered at O . Z is the effective C axis for the sample and H is the direction of the magnetic field. The angle θ is measured between the directions of H and Z , θ' between H and L . The C axes of the microcrystals constituting the sample lie within the cone with an apex angle $2\beta_0$. (b) When β is small, the base of the cone in (a) can be considered to be flat. The coordinates are then given by x and y , with E as the origin. The shaded area corresponds to the differential area having equal values of θ' .

that of the EPR lines pertaining to a single Cr ion.⁹ Accordingly, if the local C axes are not all parallel, and/or the value of D in Eq. (1) is not the same for all the Cr^{3+} ions of the sample, the sample may be viewed as being imperfect.

A. Mosaic Model

As a simple case of the imperfect sample, the sample is viewed as consisting of many *perfect* microcrystals in a mosaic form. In order to simplify the model, the following assumptions are introduced: (a) The number of Cr ions remains practically constant from one microcrystal to another. (b) The formation of the mosaic is such that, when drawn from a common origin in space, the unit vectors along the C axes of the microcrystals lie within an axially symmetric cone whose aperture angle $2\beta_0$ is very small. (c) The unit vectors are distributed symmetrically about the axis of the cone, and the angular deviation β of individual unit vectors from the cone axis may be described in terms of a Gaussian distribution with a suitable standard deviation $\Delta\beta$, which is much smaller than β_0 . The cone axis is then taken to represent the *effective* C axis of the imperfect sample. Thus, a perfect sample corresponds to the case where β_0 vanishes.

Let the cone axis (representing the effective C axis) be the polar axis of a right-handed coordinate system.

⁹ Since the x value is less than 0.001%, the line broadening due to the spin-spin interactions among the Cr ions is insignificant, as mentioned in the Introduction. Then, the linewidth is very likely to be determined by the hyperfine interactions.

Then, a unit vector (representing a local C axis) lying in the cone can be specified in terms of a polar angle β and an azimuthal angle ψ in this frame of reference. According to assumption (c), the probability of the unit vector (β, ψ) lying within a differential solid angle $d\Omega$ in the direction of (β, ψ) may be written as follows:

$$P(\beta)d\Omega = B \exp[-\beta^2/2(\Delta\beta)^2] \sin\beta d\beta d\psi, \quad (3)$$

where B is a normalization constant for the Gaussian distribution. Now let the angles that the magnetic field makes with the polar axis and with the unit vector (β, ψ) be θ and θ' , respectively, as shown in Fig. 2(a). Since β_0 is assumed very small, the surface formed by the intersection of the cone and a unit sphere centered at O may be taken to be practically flat. The coordinate system shown in Fig. 2 (b) may then be used to express $P(\beta)d\Omega$ in terms of $\theta - \theta'$, by using the following approximations:

$$\beta^2 = x^2 + y^2, \quad (4)$$

$$d\Omega \approx \beta d\beta d\psi = dx dy, \quad (5)$$

$$x = \theta' - \theta, \quad (6)$$

and also using the assumed Gaussian distribution of β :

$$P(\theta' - \theta)d\theta' = C \exp[-(\theta' - \theta)^2/2(\Delta\beta)^2]d\theta', \quad (7)$$

where $\Delta\beta$ is the half-width at maximum slope of the distribution of β .

The use of the isofrequency curves

$$\theta = f(H) \quad (8)$$

makes it possible to transform $P(\theta' - \theta)d\theta'$ into

$$P(H' - H_E)dH' = C \exp\{-[f(H') - f(H_E)]^2 \times [2(\Delta\beta)^2]^{-1}\} (df/dH')dH', \quad (9)$$

where H_E is the position of resonance for θ .

If the shape of the EPR line E for a single Cr ion in a perfect crystal is given by $g(H - H_E)$, the shape of the "composite" line E for the mosaic sample will be given by

$$G(H - H_E) = \int g(H - H')P(H' - H_E)dH'. \quad (10)$$

It is easily seen that G is dependent on the isofrequency curve of the EPR line E . Because of assumption (c), $P(H' - H_E)$ is appreciable only when the difference h between H' and H_E is small. Accordingly, $f(H')$ and df/dH' in Eq. (9) may be expanded in powers of h in the vicinity of H_E . If the derivatives of orders higher than 1 are neglected, Eq. (10) can be written as follows:

$$G(H - H_E) = C \int g(H - H_E - h) \times \exp[-h^2(f')^2/2(\Delta\beta)^2]f'dh, \quad (11)$$

where $f' = d\theta/dH$. Since the EPR line E for each microcrystal is primarily broadened by the hyperfine inter-

actions,^{2,9} the shape function $g(H-H_E)$ for the line is very likely to be Gaussian.¹⁰ If, then, g is taken to be Gaussian with a half-width Δg at the maximum slope, the shape $G(H-H_E)$ of the "composite" E is also a Gaussian, with the full width $2\Delta G$ at maximum slope.

$$2\Delta G = 2[(\Delta g)^2 + (f')^{-2}(\Delta\beta)^2]^{1/2}. \quad (12)$$

Experimentally, $2\Delta G$ is measured, and f' obtained from the isofrequency plot for individual EPR lines. If the line is Gaussian, and the value of Δg is available, then Eq. (12) yields the value of $\Delta\beta$, which is a measure of the mosaic model.

B. Strain Model

As another simple case of the imperfect sample, the sample may be such that D of Eq. (1) varies from site to site of the Cr ions, while the variation of the local C axis orientation is insignificant. The small deviation of D from the value of D in the perfect sample may be described in terms of an additional term in the spin Hamiltonian [Eq. (1)]

$$\mathfrak{H}' = \sum_{i,j} D_{ij} S_i S_j, \quad (13)$$

where the D_{ij} depend on the strain constants at local Cr sites.¹¹ The Cartesian components S_i of \mathbf{S} have the same reference system as used in Eq. (1). When the strain term \mathfrak{H}' is treated as a first-order perturbation to the Eq. (1), the resonant-magnetic-field value can be given as

$$H' = H + \sum_{ij} D_{ij} \left\{ \langle a | S_i S_j | a \rangle - \langle b | S_i S_j | b \rangle \right\} \frac{dH}{d(E_a - E_b)}, \quad (14)$$

where a and b label the levels of the Cr ion between which the transition takes place. The distribution of H' in the vicinity of H is determined by the distribution of the D_{ij} . Thus, one sees the possibility of a broadening of the line due to local strains.

If, for simplicity, the distributions of the D_{ij} 's are assumed to be all Gaussian and independent of one another, the resulting full width at maximum slope due to strain alone would be given by

$$2\Delta H_s = 2 \left[\sum_{ij} \sigma_{ij}^2 \left\{ \langle a | S_i S_j | a \rangle - \langle b | S_i S_j | b \rangle \right\}^2 \times \left(\frac{dH}{d(E_a - E_b)} \right)^2 \right]^{1/2}, \quad (15)$$

where the σ_{ij} are the half-widths at maximum slope of the distributions of the D_{ij} in energy units.

The strain broadening and the hyperfine broadening, mentioned in the Introduction, are statistically inde-

pendent in the present approximation and their effects should be added in the root-mean-square fashion. The full width at maximum slope would then be given by

$$2\Delta G = 2[(\Delta g)^2 + (\Delta H_s)^2]^{1/2}. \quad (16)$$

C. Hybrid Model

The two preceding models may be combined to form a third model under the following assumptions. Each microcrystal of the mosaic model is now subject to random local strains as in the strain model. A first approximation to the resulting linewidth of such a model would be to treat both mosaic and strain effects as statistically independent. The resulting full width of the line shape would be then given by

$$2\Delta G = 2[(\Delta g)^2 + (f')^{-2}(\Delta\beta)^2 + (\Delta H_s)^2]^{1/2}. \quad (17)$$

III. EXPERIMENTAL RESULTS AND DISCUSSIONS

Single-crystal boules of $(\text{Al}_2\text{O}_3)_{1-x}(\text{Cr}_2\text{O}_3)_x$ with x values being nominally equal to 0.01%, 0.001%, and 0.0001% have been purchased from the Linde Company, East Chicago, Indiana. Cubic samples of dimensions 3 mm×3 mm×3 mm have been prepared from these boules in such a way that one of the cubic faces is normal to the C axis which has been determined by means of Laue back-scattering patterns.

EPR absorption studies of these samples have been conducted at room temperature by means of a Varian 4500-10A EPR spectrometer assembly operated at X -band microwave frequencies. The magnetic field was modulated at 100 Kc/sec, and the derivative of the bell-shaped EPR absorption curve has been recorded. The derivative traces will be referred to as the EPR lines in the following. The width of each EPR line has been measured in units of Gauss between the two peaks of the derivative. The angular dependence of the EPR lines has been investigated by rotating the samples about the a axis perpendicular to the C axis as well as to the magnetic field. The angle of rotation θ is measured from the C axis to the magnetic field.

The curves in Fig. 1 represent the isofrequency curves (H versus θ) which have been obtained experimentally from a sample with an x value equal to 0.001%. At $\theta=0^\circ$, for example, only three lines are observable, and their widths are 11, 12.3, and 12.4 G for the lines ($1 \rightarrow 3HF$), ($1 \rightarrow 3LF$), and ($1 \rightarrow 2$), respectively.

The dependence of the measured width of individual EPR lines on θ is illustrated by the heavy solid curves connecting the vertical bars in Fig. 3. The ordinate and abscissa represent the width and the angle of rotation, respectively. Over the 90° range of θ , the width varies substantially, and its angular dependence is different for different lines. The shape of individual lines has been found to be approximately Gaussian except for a few orientations. The observed linewidth variation has been

¹⁰ For example, A. M. Portis, Phys. Rev. **91**, 1071 (1953).

¹¹ As for the general dependence of the D tensor on the stress components see P. L. Donoho, Phys. Rev. **133**, A1080 (1964).

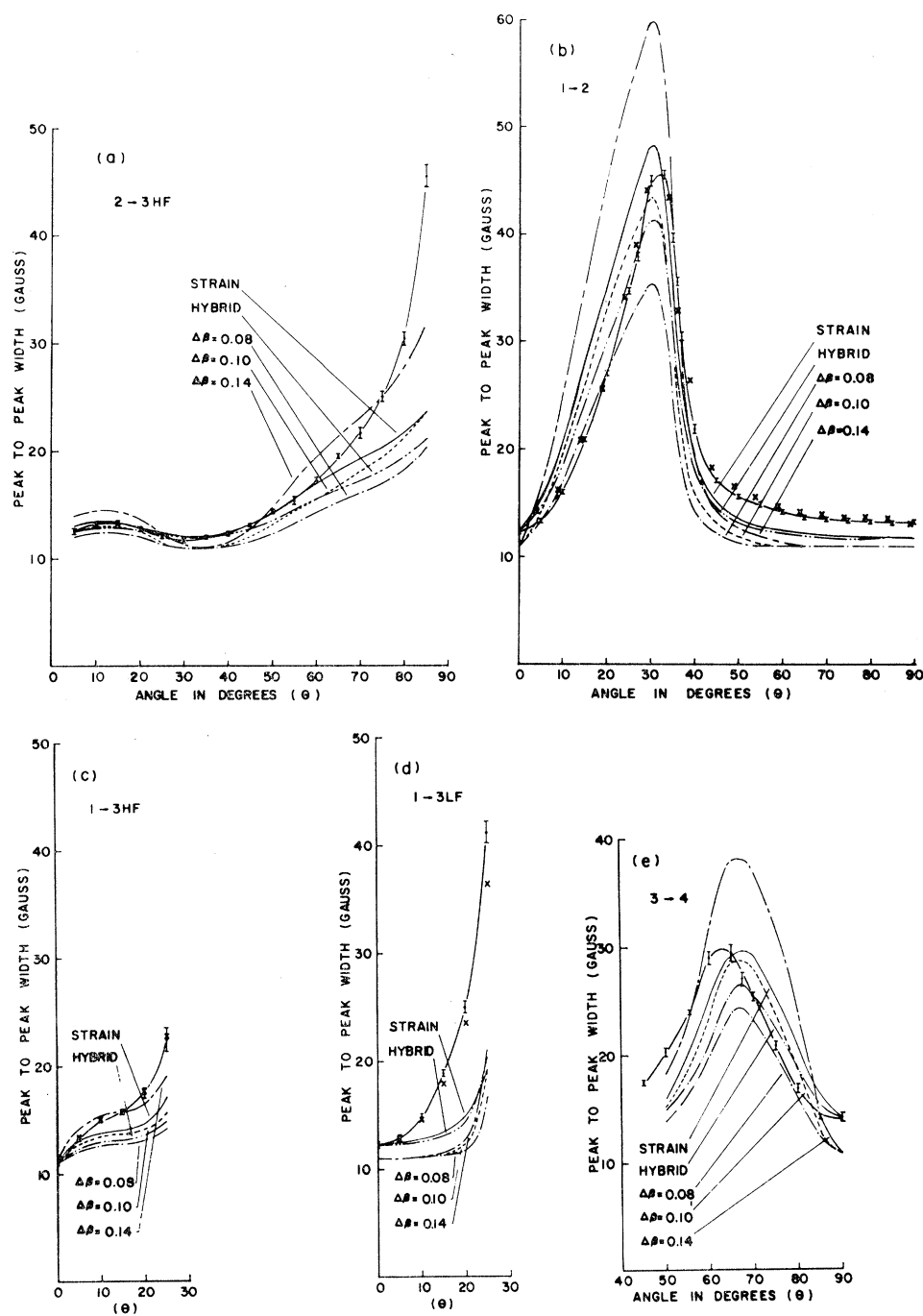


FIG. 3. A comparison of the observed and calculated angular dependences of the EPR linewidth. For example, (b) illustrates the comparison for the transition (1-2). The observed angular dependence is indicated by the solid curve joining the "error bars" (for $x=0.001\%$) and the crosses (for $x=0.01\%$), while the calculated angular dependence is indicated by the other curves based on the mosaic model with varying $\Delta\beta$, the strain model, and the hybrid model.

found to be virtually independent of the different choice of a axes, and crystal boules of different x value. Thus, the width variation seems to be a general property of low Cr-concentration samples. To illustrate the concentration independence, the linewidth data taken of a sample with $x=0.01\%$ is shown by crosses in Figs. 3(b), (c), and (d).

The linewidth variation of the line ($2 \rightarrow 3LF$) has not been investigated in the present work. This is

because the line overlaps a line belonging to the impurity Fe^{3+} spectrum for almost the entire range of θ , and the overlap is serious enough to make linewidth data for the ($2 \rightarrow 3LF$) line meaningless.

The value of Δg in Eqs. (12), (16), and (17) has been chosen to be one-half of the full width (11 G) of the line ($1 \rightarrow 3HF$) at $\theta=0^\circ$. The following reasons may be cited for choosing this value of Δg . First, $(1/f') = dH/d\theta$ vanishes at $\theta=0^\circ$, and accordingly the mosaic effect does

not contribute to the linewidth. *Secondly*, the line at this orientation corresponds to the transition ($\frac{1}{2} \rightarrow -\frac{1}{2}$) and consequently, $[\langle \frac{1}{2} | S_i S_j | \frac{1}{2} \rangle - \langle -\frac{1}{2} | S_i S_j | -\frac{1}{2} \rangle]$ vanishes for all i, j , and thus the strain effect also gives no contribution to the linewidth. However, for the other lines at $\theta=0^\circ$, which correspond to ($\frac{3}{2} \rightarrow \frac{1}{2}$) transitions, the matrix elements of $S_i S_j$ do not vanish. Therefore, the chosen width of 11.0 G is expected to be the closest to the width of the line for a perfect sample.

In order to apply Eq. (12), which gives the contribution of the mosaic model alone, the first derivative $dH/d\theta=(f')^{-1}$ has been evaluated by means of the isofrequency curves $\theta=f(H)$ in Fig. 1. Three values of $\Delta\beta$, 0.08° , 0.10° , and 0.14° have been chosen to compute the angular dependence of the linewidth predicted by Eq. (12). The calculated values are represented by the curves with $\Delta\beta$ values indicated in Fig. 3. Of the three alternative values of $\Delta\beta$, the case of $\Delta\beta=0.10^\circ$ seems to yield the optimum fitting to the observed curves.

To evaluate the linewidth variation due to the strains by means of Eqs. (15) and (16), the eigenfunctions of Eq. (1) have been obtained as a function of θ by means of a computer and the matrix elements of $S_i S_j$ evaluated for the appropriate levels represented by the eigenfunctions. The value of $dH/d(E_a-E_b)$ has been obtained by similar computational methods.

Because of the axial symmetry of Eq. (1), and the fact that the value of D_{yy} can be subtracted from all the diagonal elements of D_{ij} without change in the relative spacing of the magnetic levels, the only matrix elements that contribute to Eq. (15) are S_x^2 , S_z^2 , and $(S_x S_z + S_z S_x)$. A Gaussian distribution has been assumed for each of D_{xx} , D_{zz} , and $D_{xz}(=D_{zx})$, and the half-widths, σ_{xx} , σ_{zz} , and σ_{xz} of these distributions have been treated as adjustable parameters. The solid curves labeled "strain" in Fig. 3 represent the calculated linewidth variation of the strain model obtained by the optimum values of the parameters,

$$\begin{aligned} \sigma_{xx} &= 6.25 \text{ Mc/sec}, & \sigma_{zz} &= 2.25 \text{ Mc/sec}, \\ \sigma_{xz} &= 10.6 \text{ Mc/sec}. \end{aligned} \quad (18)$$

In using the hybrid model [Eq. (17)], the following optimum value for the parameters were used:

$$\begin{aligned} \sigma_{xx} &= 6.25 \text{ Mc/sec}, & \sigma_{zz} &= 2.25 \text{ Mc/sec}, \\ \sigma_{xz} &= 3.85 \text{ Mc/sec}, & \Delta\beta &= 0.08^\circ. \end{aligned} \quad (19)$$

The linewidth variation computed from Eqs. (15) and (17) with these values of the parameters is illustrated by the curves labeled "hybrid" in Fig. 3.

A survey of Fig. 3 indicates that all of the three proposed models qualitatively predict the observed linewidth variation, and that the strain model is the best of the three. None of the models, however, predicts quantitatively the variation over the entire range of θ . This failure is particularly severe in the region around $\theta=25^\circ$ for the ($1 \rightarrow 3HF$) and ($1 \rightarrow 3LF$) transitions, and around $\theta=85^\circ$ for the ($2 \rightarrow 3HF$) transition. Also,

the ($3 \rightarrow 4$) transition shows the anomaly that the peak predicted by all three models is displaced from that of the experimental peak by about 5° . Repeated experimental investigations of the peak region have failed to eliminate the shift of the peaks.

A few possible causes may be speculated for the lack of quantitative agreement between the theoretical predictions and the experimental results in some angular regions.

First, two points pertaining to the mosaic model should be re-examined: (i) The formation of the mosaic in the samples might not be "random."¹² If this is the case, the cone in Fig. 2(a) would not be axially symmetric, and accordingly, different choices of the a axis of rotation would yield different linewidth variations. Experimentally, however, no dependence of the linewidth variation on the choice of a axis has been noticed (see Sec. III). (ii) The neglect of the derivatives of $\theta=f(H)$ of order higher than the first might not be proper in obtaining Eq. (11). A discouraging consequence of including the higher order derivatives in Eq. (11) is that the second factor in the integrand becomes non-Gaussian and consequently the shape of G would deviate from the Gaussian shape. Experimentally, however, the observed shape of G is practically Gaussian, except for a few orientations, as mentioned in Sec. III. Therefore, it appears that the simple mosaic model used in the present work is not mainly responsible for the quantitative discrepancy between the experimental and calculated results. It is interesting to note here that a mosaic model similar to the present one has been successfully employed by Shaltiel and Low for the case of Gd ions in ThO_2 ,³ and the value of $\Delta\beta$ based on the former model is similar to that of $\Delta\beta$ obtained from the present model. There is also evidence in support of the actual mosaic formation of single crystals of Al_2O_3 ,¹² which would correspond closely to the samples investigated in the present work.

Secondly, it is true that the strains characterized by D_{ij} in Eq. (14) are of a special nature, which would correspond to the case of an axially symmetric distribution of strains at each Cr site. Two types of strains which are a little more general than the one used in the present strain model may be considered: (i) The strains are such that the local C axis is also "tipped" from its direction in a perfect sample. This case is very similar to the hybrid model used in the present work (see Sec. II C). However, as one can see from Fig. 3, the hybrid model is less successful than the strain model. (ii) The strains are such that the local C axis can no longer be defined. For this case, the spin Hamiltonian itself given by Eq. (1) is inadequate, because the axial symmetry of the D tensor is no longer valid. This type of strain is expected to originate more in samples of Cr-concentrations much larger than 0.01%. So far, however, the spin Hamiltonian given by Eq. (1) has

¹² D. L. Stephens and W. J. Alford, J. Am. Ceram. Soc. 47, 81 (1964).

been found to be satisfactory even for samples of larger concentrations.⁷

Thirdly, in the case of the strain model, the g values have been taken to remain the same from one site of Cr ion to another. Strictly speaking, this is not valid, because a variation of the strain parameters is related to a variation of g value.¹³ Recently, Scott *et al.*, have reported on EPR line broadening due to the g value variation in rare-earth salts.¹⁴ This mechanism, however, does not appear to be noticeably effective for the Cr³⁺ ions investigated in the present work (see Appendix I). Nevertheless, possible effects of varying the g values depending on different sites of the ions have been investigated by means of a computer. The results of the investigation, however, have indicated that the anisotropy of the linewidth based on the g -value variation is not consistent with the observed anisotropy at all.

Thus, it appears that the quantitative discrepancy between the observed and calculated results in Fig. 3 is not due to the simple nature of the models used in the present work. But some other causes are probably responsible, at least in part, for the discrepancy. In this respect, it is interesting to note that some workers have recently encountered somewhat similar situations.^{3,4}

V. CONCLUSION

The angular dependence of the width of the EPR lines of the samples of $(\text{Al}_2\text{O}_3)_{1-x}(\text{Cr}_2\text{O}_3)_x$ with x less than 0.01% have been investigated by rotating the samples about an axis perpendicular to the C axis of the samples. The observed anisotropy of the width varies from one EPR line to another. The width varies by more than a factor of 5 over the 90° range of the angle of rotation. Such variation of the width is not easily explained in terms of only the hyperfine interactions of Cr ions with the neighboring Al ions.

To account for the observed linewidth variation, three alternative models have been employed: The mosaic model, the strain model, and the hybrid model. The linewidth variation predicted by each of the models agrees qualitatively with the observed linewidth varia-

tion. Of the three models, the strain model seems to be the best. Quantitatively, however, the models are not satisfactory particularly in some angular regions.

Re-examination of the basic assumptions pertaining to the individual models in reference to the experimental results seems to suggest that the quantitative discrepancy between the observed and calculated results is not due to the defects of the individual models. It is probably, at least in part, due to some causes which are different in nature from the mechanisms considered in the present work.

ACKNOWLEDGMENT

The authors would like to express their thanks to the Wayne State University Computing and Data Processing Center, Detroit, Michigan, for the use of the IBM 7070 computer.

APPENDIX: G-VALUE VARIATION

An approximate relation between the spin-orbit coupling constant λ and the experimentally measured parameters D , g_{11} , and g_{\perp} , can be given as follows¹⁵:

$$D \simeq \frac{1}{2}\lambda(g_{11} - g_{\perp}). \quad (\text{A1})$$

Using the values of Eq. (2) of the present article

$$\lambda \simeq 4 \times 10^6 \text{ Mc/sec}. \quad (\text{A2})$$

Considering the variation of g_{11} and g_{\perp} to be mutually independent as they are determined by the assumed independent components of D_{ij} , an order of magnitude estimate of the half-width of the variation of either g_{11} or g_{\perp} can be given by

$$\delta g \simeq (\delta D / \lambda), \quad (\text{A3})$$

where δD is the half-width of the variation of D .

By using the maximum value of δD (10.6 Mc/sec) in the present article, a value of $\delta g = 0.3 \times 10^{-5}$ is thus obtained. The magnitude of the line broadening due to this value is estimated by

$$\Delta H = (dH/dg)\delta g. \quad (\text{A4})$$

The largest value of dH/dg obtained by means of a computer is 3.82×10^3 G/unit g for the 1-2 line at $\theta = 0^\circ$. Consequently, ΔH is at most 0.01 G. This is too small to be significant when compared with the line broadening estimated by using the strain model.

¹³ See, for instance, W. Low, in *Solid State Physics*, edited by F. Seitz and D. Turnbull (Academic Press Inc., New York, 1960), Suppl. 2, p. 82.

¹⁴ P. L. Scott, H. J. Stapleton, and C. Wainstein, *Phys. Rev.* **137**, A71 (1965).